

# PERFORMANCE OF A HIGH-POWER, 2.388-GHz RECEIVING ARRAY IN WIRELESS POWER TRANSMISSION OVER 1.54 km

Richard M. Dickinson

Jet Propulsion Laboratory, California Institute of Technology  
Pasadena, California

## Abstract

The results of a series of experiments conducted to determine the performance of a microwave power receiving array are detailed. Over 30 kW of dc output power has been achieved. The ratio of dc output power to available incident RF input power has exceeded 0.8. The array performance readily scales from the extrapolated single element performance.

## Introduction

Wireless power transmission [1, 2, 3] is proposed as the link from space to Earth for energy transmission from orbiting power satellites [4]. The technology also has potential applications in underground transmission of power via waveguide, rapid switching of electric power via phased array beam direction, and electric powered aircraft levitation [5]. The technology may also have potential biological impact consequences if applications are not properly designed, engineered, constructed, and controlled.

The normal operational performance and selected parameter variation characteristic curves are presented and discussed for a 24-m<sup>2</sup> area array currently being evaluated as a receiving-converting subsystem (RXCV) of a wireless microwave power transmission system. The system is being developed for NASA by JPL for the purpose of technology verification, demonstration, and advancing the state of the art in microwave power transmission.

Previous measurements of a laboratory version of a total microwave transmission system [6] had shown that relatively high (54%) overall dc input-to-output power transmission efficiency could be achieved. However, the power level was only 1/2 kW and the distance 1.7 m. Therefore, the next technology step was a check of the adequacy of scaling to a longer range, higher power level system. Thus, the Goldstone tests, as outlined in Ref. 7, were undertaken.

## RF Power Collection and Conversion Devices

The rectenna (Fig. 1), along with its equivalent circuit [8], is the basic building block of the high-power receiving array. The particular rectenna element configuration was developed by Raytheon Co. for JPL under NASA Office of Applications and Office of Energy Programs contract.

The elements consist of a GaAs rectifier diode connected via a low-pass filter to a half-wave dipole antenna. The elements are operated with the dipole spaced approximately a quarter wavelength above a ground plane. A portion of the filter, the diode, and dc leads project through a hole in the ground plane. The rectennas are dc-isolated from the ground plane to allow outputs in parallel with common buss bars and to allow groups of parallel outputs in series to raise the subarray output voltage to a working level of ~150 V.

A group of 270 rectennas in a 1.162 X 1.207-m subarray were wired with dc collection connections behind the ground plane (Fig. 2). Seventeen of the

subarrays are configured in a 3 X 6 matrix array (Fig. 3). Each subarray has its own over-voltage protective circuit, load, and instrumentation.

## Performance Test Equipment

The RXCV array is mounted approximately half-way up a 30-m tower that is separated by a 1.54-km slant range at an elevation of 7° from the 26-m-diameter parabolic antenna of the Venus station (Fig. 4), which is located at Goldstone, near Barstow, California.

The Venus station transmitter is a 2.388-GHz klystron capable of radiating up to 450 kW of CW power. Because the array is only 7.3 m high by 3.5 m wide, combined with the fact that the energy is distributed nonuniformly across the beam with peak intensity in the center and lesser amounts at the array edges, the array normally intercepts ~11.3% of the energy from the transmitter.

The instrumentation for each subarray consists of an RF input power density sample obtained by isolating the central subarray rectenna element and providing it with its own individual load, an RF shielded thermistor element affixed to the central buss bar to monitor temperature (the buss bar is the predominant mass and thus the heat sink for the rectenna diodes), and precision output voltage dividers and current shunts across each of the 17 dc output loads.

The incident RF sample diodes are individually calibrated by use of stored diode characteristics in computer software in conjunction with a calibrated gain RF horn seen at the lower right of Fig. 3.

The computer processes the measured data to display input RF power ( $\pm 2.0\%$  accuracy), dc output power ( $\pm 0.5\%$ ), and efficiency ( $\pm 2\%$ ) for each subarray and for the total array. Also, subarray temperatures ( $\pm 1^\circ\text{C}$ ) and voltages ( $\pm 0.5\%$ ) are displayed.

## Array Performance Experiments

In addition to the normal power output versus power input or efficiency measurements (Fig. 5), a series of experiments were conducted to determine the RXCV performance under various conditions to provide nonstandard operating characteristics and to pinpoint areas for improvement.

The first experiment was to vary the dc load resistance of a subarray and measure the RXCV conversion efficiency. The subarray is designed with a high impedance load to allow optimizing efficiency performance at low flux density levels and a low impedance load for safe maximum power output conditions.

A portion of the load consists of lamps in which approximately one-third of the dc power output is dissipated. By shorting out the lamps and with the high power-low power range switch, the data shown in Fig. 6 was amassed. Short-circuit current performance is given in Ref. 7.

Rectenna subarray performance as a function of angle of incidence in the E-plane is given in Fig. 7. The varying angle was achieved by tilting one of the central subarray about its lower edge with the aid of ropes and tag lines. The H-plane pattern is expected to be similar. The entire array is supported on a frame that is tilted  $7^\circ$  with respect to the collimation tower vertical in order that the subarrays will be normal to the incoming RF beam.

Figure 8 indicates the scaling performance of a subarray and the entire array relative to the performance of a single rectenna element. The curves were obtained by dividing the subarray and array power outputs by 270 and 4590, respectively, the corresponding numbers of individual rectenna elements under consideration. The calibration elements are specially selected and have slightly higher efficiency.

Testing the array performance as a function of RF frequency was restricted by the narrowband tuning characteristics of the klystron to a range of -15, +7.5 MHz. Over the frequency variation range, the conversion efficiency varied only +2, -1%, which is on the order of magnitude of the instrumentation accuracy. Thus, the bandwidth of the array remains to be determined. Nevertheless, most power transmission applications do not require significant operating bandwidth.

The polarization performance of the array could only be partially checked, as the high-power transmitter at the Venus site is equipped with only a single rotary quarter-wavelength polarizer section. Hence, only one state of linear polarization can be achieved, whereas positionable linear polarization is desired. Nevertheless, the array performance, in general, followed the theoretical  $\sec^2\theta$  polarization loss curve of the vertical linear polarized component of the polarizer angular position.

The ground plane spacing of two subarrays was varied  $\pm 0.06\lambda$ . The collection-conversion efficiency varied  $\pm 3\%$ . Thus, a more optimum ground plane spacing ( $\sim 0.26\lambda$  rather than the existing  $0.20\lambda$ ) may be appropriate.

The array has been operated at buss bar temperatures of +8 to +45°C with undetectable performance variations.

Additional tests consisted of observing the performance variations of a subarray relative to various conditions of its neighbor subarrays. For example, the collecting cross section of a single isolated subarray appears to be slightly larger than when it is surrounded by neighbors--although the accuracy is not as good as desired, since the measurements were made before the instrumentation system was completely calibrated. Short-circuiting a subarray does not appear to cause any noticeable change in an adjacent subarray output. However, it is known that when a subarray is short-circuited, the power level to the central isolated load calibration element increased by 25%.

Stepping out the axial position of a subarray by a quarter wavelength did not result in any noticeable change in the performance of the advanced position subarray or of the surrounding subarrays.

It is interesting that the overall array performance did not change when one central subarray was tilted at various angles of incidence, up to  $40^\circ$ . By observing the performance of the adjacent subarray's isolated load calibration elements, it was seen that there were local areas of enhanced and diminished RF power density of -15 and +10% due to the fields scattered from the tilted subarray. However, almost all of the scattered energy must have been absorbed by the other subarrays. Nevertheless, variations before and during tilting were almost negligible in the subarray's dc outputs, with the exception of the subarray under test.

#### Conclusions

A highly efficient, rather tolerant, nondirective RF to dc converter has been characterized over certain ranges as regards dc load, RF frequency, polarization, power density level and distribution, mechanical position, incident illumination angle, temperature, and ground plane spacing. The rectenna array has been successfully used to transfer >30 kW of power over a distance of 1.54 km with a collection-conversion efficiency >80%.

The rectenna subarray and array performance readily scales from the single element characteristics. Thus, the proposals for having billions of rectennas in either the Earth-based receiving stations of geosynchronous orbiting satellite power systems or in the intermediate and ultimate link in the sun synchronous orbit-geosynchronous orbit transponder satellites should not present a technical problem in concept.

Future rectenna developments should be in the areas of reduced production cost and extended power range capability as well as increased efficiency.

#### Acknowledgments

This paper presents the results of one phase of research carried out at the Jet Propulsion Laboratory, California Institute of Technology, under Contract NAS7-100, sponsored by the National Aeronautics and Space Administration.

#### References

1. Susskind, C., "The Early History of Electronics II. The Experiments of Hertz," *IEEE Spectrum*, Vol. 5, No. 12, Dec. 1968, pp. 57-60.
2. O'Neill, J. J., *Prodigal Genius, The Life of Nikola Tesla*, Ives Washburn, Inc., N. Y., 1944.
3. Brown, W. C., "The Technology and Application of Free-Space Power Transmission by Microwave Beam," *Proc. of IEEE*, Vol. 62, No. 1, Jan. 1974, pp. 11-25.
4. Williams, J. R., "Geosynchronous Satellite Solar Power," *Astronautics and Aeronautics*, Nov. 1975, pp. 46-52.
5. Okress, E. C., *Microwave Power Engineering*, Vols. 1 and 2, Academic Press, N. Y. 1968.
6. Dickinson, R., and Brown, W., *Radiated Microwave Power Transmission System Efficiency Measurements*, TM 33-727, Jet Propulsion Lab., Pasadena, Calif., May 15, 1975.
7. Dickinson, R., *Evaluation of a Microwave High-Power Reception-Conversion Array for Wireless Power Transmission*, TM 33-741, Jet Propulsion Lab., Pasadena, Calif., Sept. 1, 1975.
8. Nahas, J. J., "Modeling and Computer Simulation of a Microwave-to-DC Energy Conversion Element," *IEEE Trans. Microwave Theory Tech.*, Vol. MTT-23, No. 12, Dec. 1975, pp. 1030-1035.

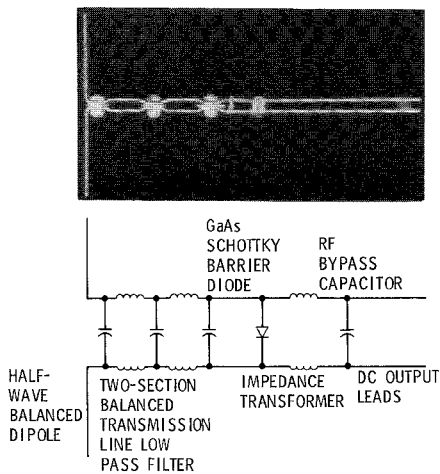


Fig. 1. Rectenna Element and Equivalent Circuit

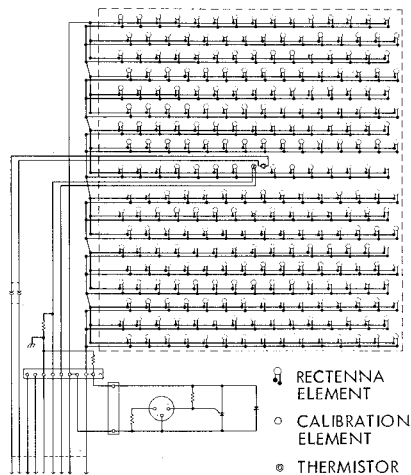


Fig. 2. Subarray Wiring Diagram

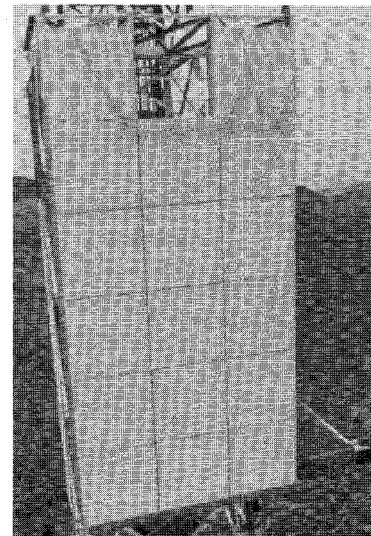


Fig. 3. The RXCV Array

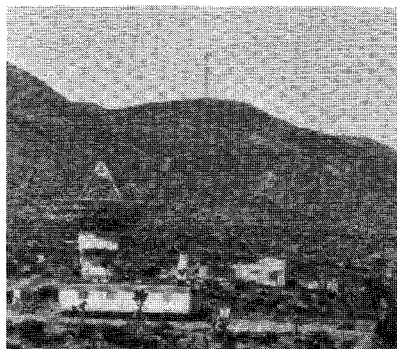


Fig. 4. The Venus Station and Collimation Tower

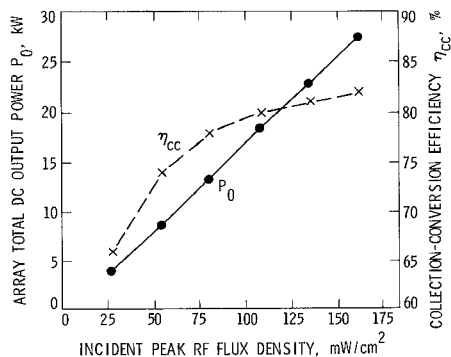


Fig. 5. Microwave High-Power Array Performance

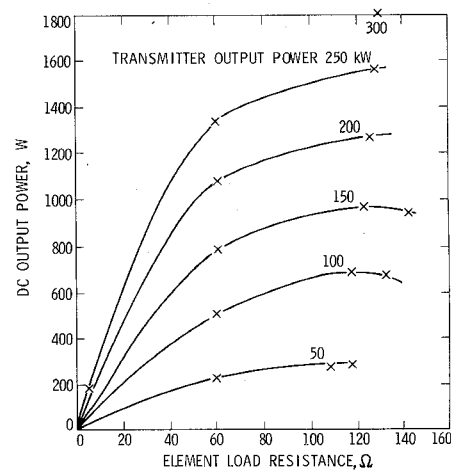


Fig. 6. RXCV Variable Load-Incident Power Characteristics

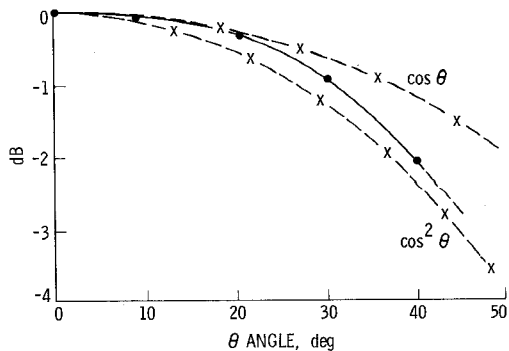


Fig. 7. Rectenna Subarray E-Plane Pattern

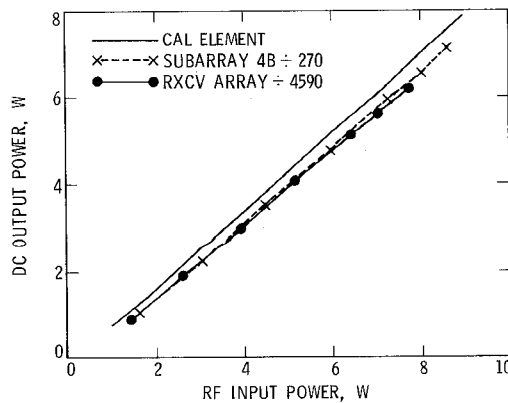


Fig. 8. Transfer Efficiency Performance Comparison